Contriving Gel Polymer Electrolyte to Drive Quasi-Solid-State High-Voltage Li Metal Batteries at Ultra-Low Temperatures

Xuanfeng Chen[a], Chunhao Qin[a], Fulu Chu[a], Fangkun Li[b], Jun Liu[b], Feixiang Wu*[, a]

[a] National Engineering Research Centre of Advanced Energy Storage Materials, School of Metallurgy and Environment, Central South University, Changsha 410083, PR China.

[b] Guangdong Provincial Key Laboratory of Advanced Energy Storage Materials, School of Materials Science and Engineering, South China University of Technology, Guangzhou, 510641, China.

*Corresponding authors: Feixiang Wu (feixiang.wu@csu.edu.cn);

Experimental Section

Materials

$LiNi_{0.8}Co_{0.1}Mn_{0.1}O_2$ (NCM811) and $LiCoO_2$ (LCO) powders were obtained from Shanghai Shanshan Technology Co., Ltd. Li foils (99.95%) were processed into two thickness of 50 and 450 μm (China Energy Lithium Co., Ltd). N-methyl-2-pyrrolidone (NMP, anhydrous), Lithium Tetrafluoroborate ($LiBF_4$, 99.9%), Fluoroethylene Carbonate (FEC, 99.9%), 1,3-Dioxolane (DOL, 99.9%) and the reference carbonate electrolyte (i.e., 1 M $LiPF_6$ in EC: DEC 1: 1 v/v) were purchased from DoDo Chem Co., Ltd.

Electrode fabrication

Typically, 80 wt% active materials (NCM811 or LCO), 10 wt% Super-P and 10 wt% PVDF were uniformly dispersed in the NMP solvent to form slurry. Then, the slurry was cast on Al foil as a current collector and dried at 80 °C for 12 hours in a vacuum. The mass loading ~3 mg cm^{-2} or 10 mg cm^{-2} of two kinds of cathodes was adjusted by coating thickness. For coin cells, the cathodes were cut into 12mm diameter with a mass loading of 3 mg cm^{-2}. The thickness of Li anode was 450 μm. For pouch cells, the cathodes were cut into 43 mm× 56 mm with a mass loading of 10 mg cm^{-2}. The thickness of Li anode was 50 μm. And the electrolyte to capacity (E/C) ratio is 2 g Ah^{-1}.

Gel polymer electrolyte (GPE) preparation

GPE (2 M $LiBF_4$ in FEC: DOL 1: 9 v/v) is composed of solute $LiBF_4$ (as salt and initiator), solvent DOL (as monomer) and organic solvent FEC. Firstly, $LiBF_4$ and FEC were well-mixed according to stoichiometry. Then, DOL was subsequently added in the mixture. Finally, $LiBF_4$ was completely dissolved with stirring to obtain the precursor solution. The precursor solution was prepared in a glovebox (MIKROUNA) with an inert atmosphere (high purity argon, 99.9%; H_2O < 0.1 ppm; O_2 < 0.1 ppm). Significantly, the precursor solution would polymerize in an hour at room temperature.

Materials characterizations

The precursor solution and polymer electrolyte were dissolved in Dimethyl sulfoxide-d6 for ^1H and ^{13}C Nuclear magnetic resonance (NMR) analysis on Bruker AVANCE III 500M. Fourier transform

infrared (FT-IR) spectra of the precursor solution and polymer electrolyte were characterized by Thermo Scientific, Nicolet iS50. The GPE was dissolved in tetrahydrofuran for gel permeation chromatograph (GPC) on Agilent GPC 50. Differential Scanning Calorimetry (DSC) (NETZSCH DSC214) was employed to investigate the glass transition temperature and the melting temperature of GPE, the test temperature range is -80 °C to 120 °C, and the heating rate is 10 °C min^{-1}. Thermogravimetry (TG)-DSC (NETZSCH STA2500) was used to test the thermal stability of GPE from room temperature to 250 °C, and the heating rate is 10 °C min^{-1}. In the Atomic Force Microscopy (AFM, Bruker DIMENSION ICON with a Nanoscope V controller) experiment, the Peak Force Tapping (PFT) mode was used to detect the morphology of the polymer electrolyte. X-ray photoelectron spectroscopy (XPS) was carried out on Thermo Fisher Scientific ESCALAB250Xi. Time of Flight Secondary Ion Mass Spectrometry (TOF-SIMS) with negative mode was operated on TESCAN GAIA3. The high-resolution transmission electron microscopy (HRTEM) images of cycled cathodes were conducted on FEI Tecnai G2 F30.

Electrochemical characterization

Galvanostatic charge/discharge tests of batteries were recorded by LAND-CT3001A battery systems. Electrochemical impedance spectroscopy (EIS) for ionic conductivity (σ) was performed by an electrochemical workstation (Gamry, Interface-1000E), where the frequency range was from 1 MHz to 0.1 Hz and the amplitude voltage was 10 mV. Stainless steel (SS)||SS symmetric cells with GPE membrane were used to measure impedance (R) and obtain ionic conductivities (σ) from −20 to 45 °C. The ionic conductivities (σ) of the GPE were calculated by the following Equation (1):

$$\sigma = \frac{l}{SR} \tag{1}$$

where l (cm) is the thickness of the GPE, S (cm^2) is the contact area with the SS, and R (Ω) is recorded from EIS. In this work, the l and S of the GPE are 0.15 cm and 0.5024 cm^2, respectively. To evaluate the electrochemical stability window of the GPE, linear sweep voltammetry (LSV) was conducted on Li||SS coin cells with a voltage scan rate of 1 mV s^{-1} from 3 to 5.5 V (Gamry, Interface-1000E). To evaluate the exchange current density, LSV (Gamry, Interface-1000E) was performed on Li||Li symmetric cells with a voltage scan rate of 1 mV s^{-1} from -0.2 to 0.2 V. The Li-ion

transference number (t_{Li^+}) of the GPE was calculated by chronoamperometry (CA) with a DC polarization voltage (ΔV) of 10 mV and EIS of Li||Li symmetric cells (Gamry, Interface-1000E). The t_{Li^+} of the GPE was calculated according to Equation (2):

$$t_{Li^+} = \frac{I_s(\Delta V - I_0 R_0)}{I_0(\Delta V - I_s R_s)} \quad (2)$$

where I_0 and I_s are the initial and steady currents during polarization, R_0 and R_s are the initial and steady interfacial resistances, respectively. To estimate the impedance of Li||NCM811 coin cells used of GPE or reference carbonate electrolyte, EIS was recorded with a frequency range from 1 MHz to 0.01 Hz. Cyclic voltammetry (CV) tests were conducted with Li||NCM811 coin cells at a scanning rate of 0.1 mV s^{-1} (Gamry, Interface-1000E). The electrochemical floating experiments were conducted on Li//NMC811 cells to obtain the leakage currents of the GPE and LE at -20 °C, which were charged to 4.0 V first, then held at progressively higher voltages with a DC ΔV of 10 mV, each for a period of 10 h.

Computational Methods

Quantum chemistry calculations were first performed to optimize molecular geometries of DEC, DOL, EC, and FEC solvent molecules using the Gaussian 16 package [Gaussian-16] at B3LYP/6-311+G(d,p) level of theory. A polymerized DOL chain consisting of 4 DOL monomers was constructed and optimized at the same level of theory. The atomic partial charges on these solvent molecules were calculated using the ChelpG method at the same level of theory (the B3LYP hybrid functional and the 6-311+G(d,p) basis set). The atomistic force field parameters for all ions (Li+, BF4- and PF6-) are described by the AMBER format and are taken from a previous work [amber-ff]. The cross-interaction parameters between different atom types are obtained from the Lorentz-Berthelot combination rule.

Three modelling systems were constructed, and the detailed system compositions are listed in Supplementary Table 2. All atomistic simulations were performed using GROMACS package with cubic periodic boundary conditions [gromacs]. The equations for the motion of all atoms were integrated using a classic Verlet leapfrog integration algorithm with a time step of 1.0 fs. A cutoff radius of 1.6 nm was set for short-range van der Waals interactions and real-space electrostatic

interactions. The particle-mesh Ewald (PME) summation method with an interpolation order of 5 and a Fourier grid spacing of 0.20 nm was employed to handle long range electrostatic interactions in reciprocal space. All simulation systems were first energetically minimized using a steepest descent algorithm, and thereafter annealed gradually from 600 K to room temperature (300 K) within 10 ns. All annealed simulation systems were equilibrated in an isothermal-isobaric (NPT) ensemble for 20 ns of physical time maintained using a Nosé-Hoover thermostat and a Parrinello-Rahman barostat with time coupling constants of 0.4 and 0.2 ps, respectively, to control the temperature at 300 K and the pressure at 1 atm. Atomistic simulations were further performed in a canonical ensemble (NVT) for 50 ns, and simulation trajectories were recorded at an interval of 100 fs for further structural and dynamical analysis.

Representative solvation structures were extracted from extensive atomistic simulations, and these solvation structures were adopted as starting configurations for additional DFT calculations. DFT calculations were performed using the Gaussian 16 software [gaussian] at the same level of theory (B3LYP/6-311+G(d)) and with Grimme's-D3 (gd3bj) dispersion correction to obtain the corresponding LUMO-HOMO energies and molecular electrostatic potential contours.

Figures and Tables

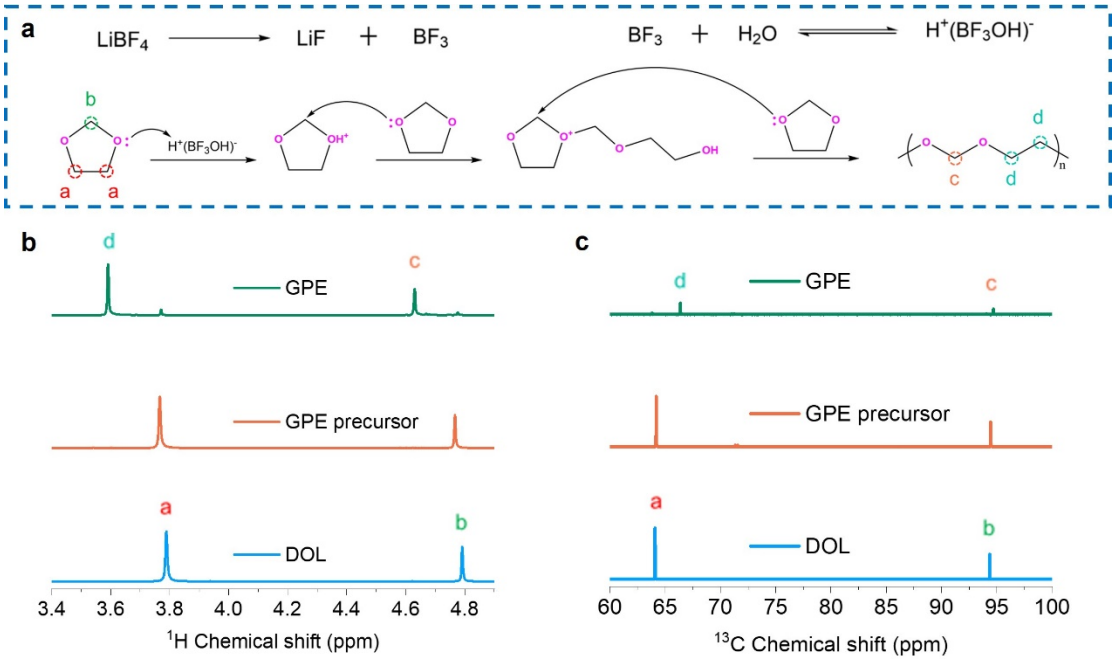

Fig. S1 a) Reaction mechanism between DOL and $LiBF_4$. The **b**) ^{1}H NMR spectra and **c**) ^{13}C NMR spectra of pure monomer DOL, the GPE precursor and the GPE.

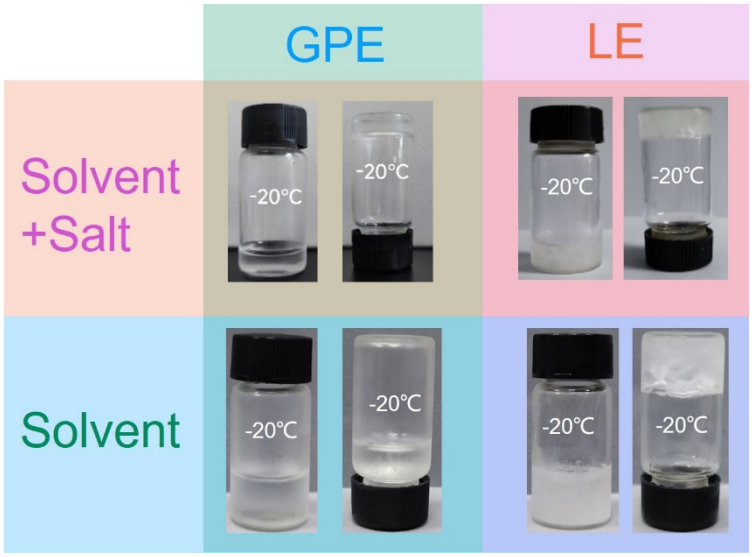

Fig. S2 The optical photos of two electrolytes (GPE: 2 M $LiBF_4$ in FEC: DOL 1: 9 vol%:vol%; LE: 1 M $LiPF_6$ in EC: DEC 1: 1 vol%:vol%) at -20 °C.

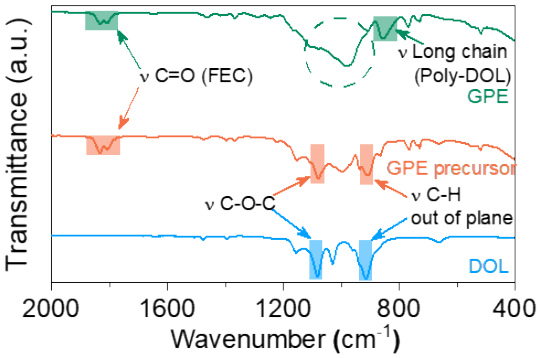

Fig. S3 The FT-IR spectra of pure monomer DOL, the GPE precursor and the GPE.

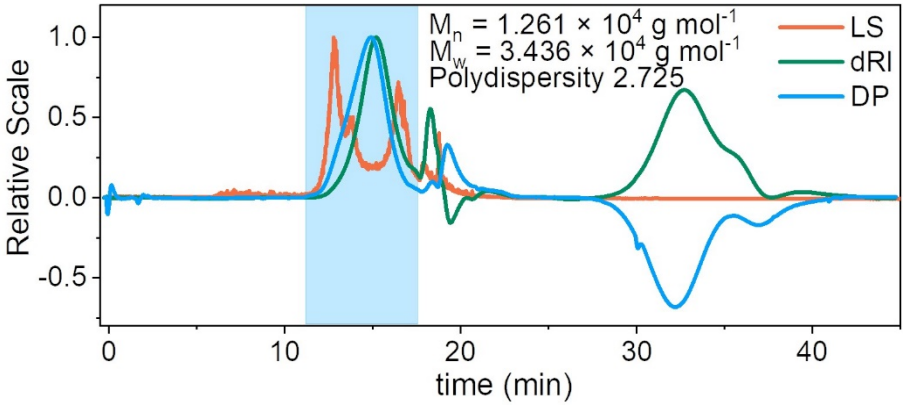

Fig. S4 M_n, M_w and PDI values of the GPE.

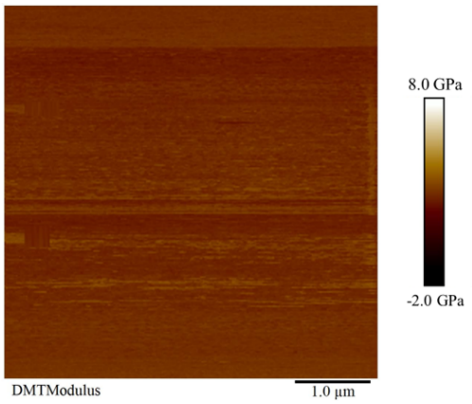

Fig. S5 Young's Modulus on the surface of the GPE.

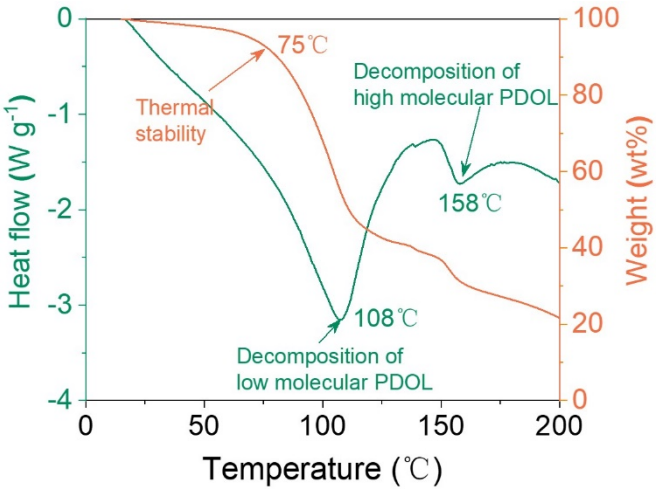

Fig. S6 TGA and DTG curves of the GPE.

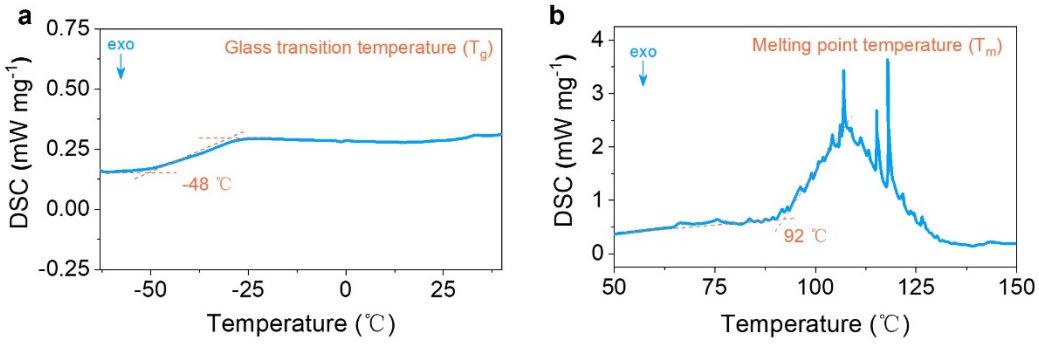

Fig. S7 DSC curves of the GPE to obtain the **a**) T_g and **b**) T_m.

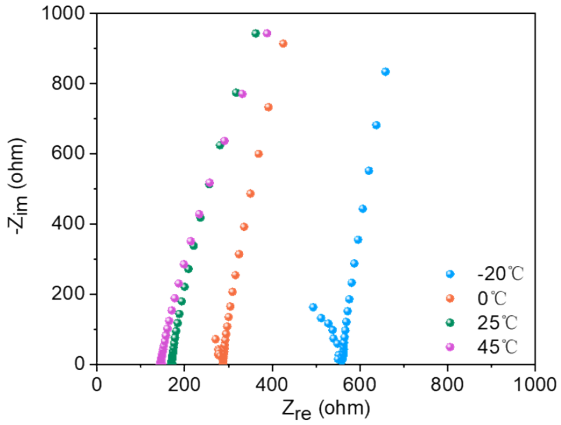

Fig. S8 EIS measurements of the GPE at various temperatures using a stainless steel||stainless steel cell.

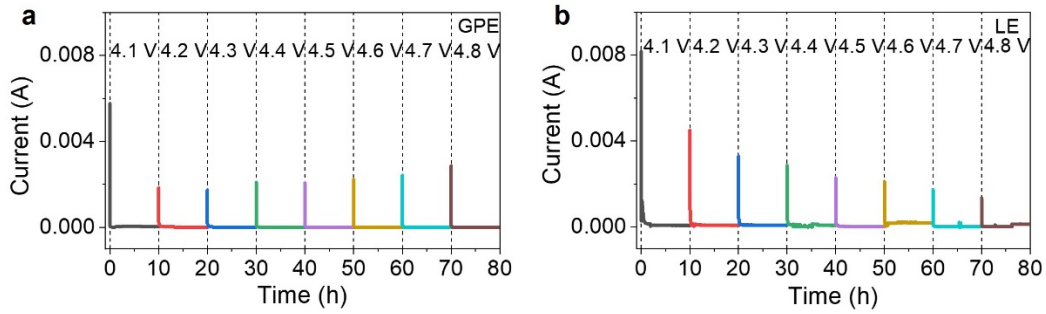

Fig. S9 Electrochemical floating analysis of the **a**) GPE and **b**) LE using NCM811 cathodes at -20 °C.

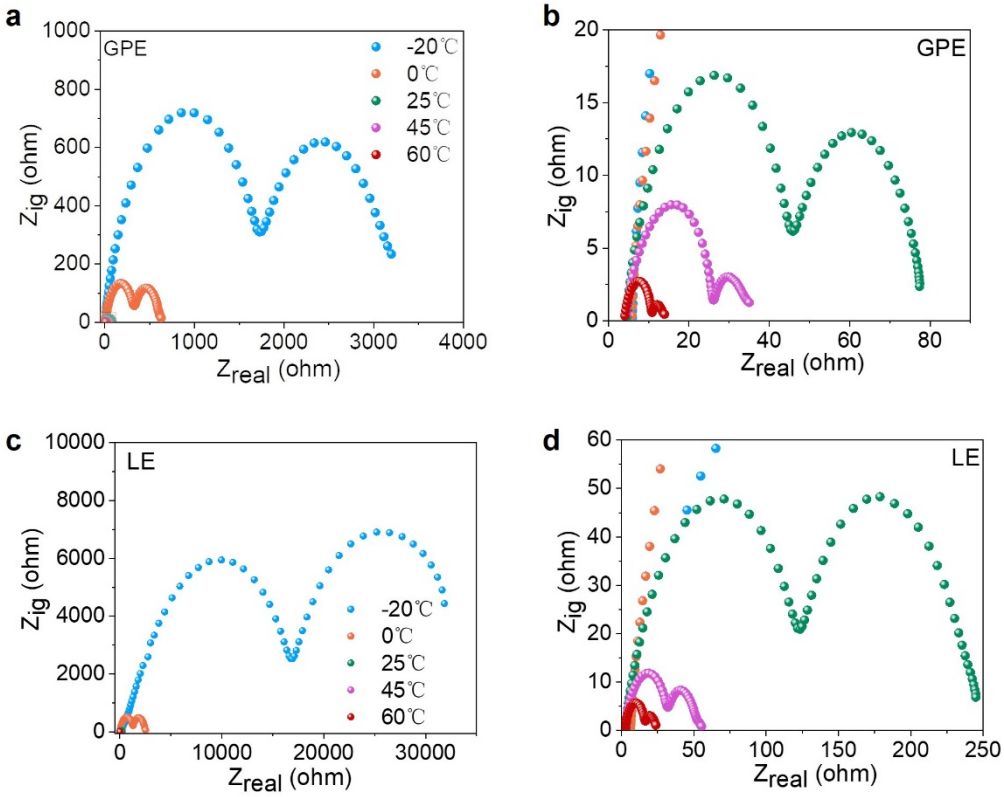

Fig. S10 EIS measurements of the **a**) GPE and the **c**) LE at various temperatures using a Li|| Li cell. **b**), **d**) The magnification of (**a**) and (**c**).

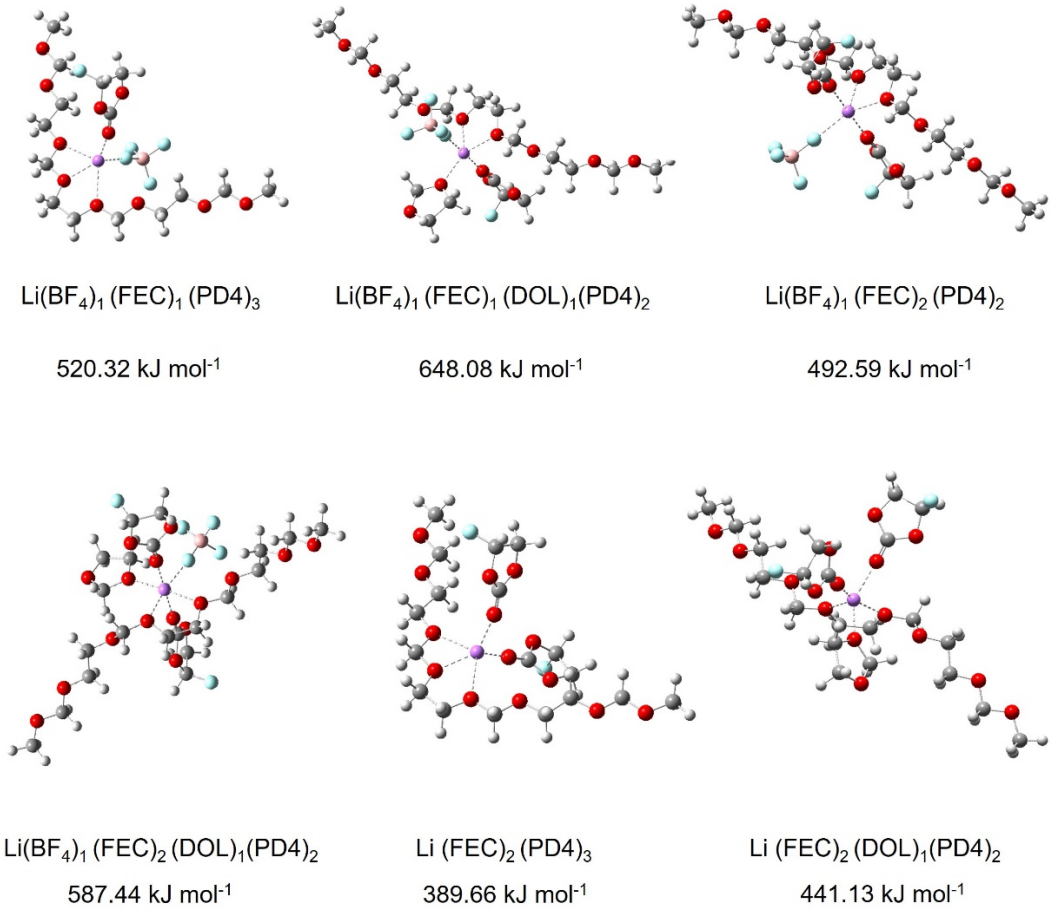

Fig. S11 The representative Li^+ solvation structures in the GPE and their desolvation energy at -20 °C via DFT calculation.

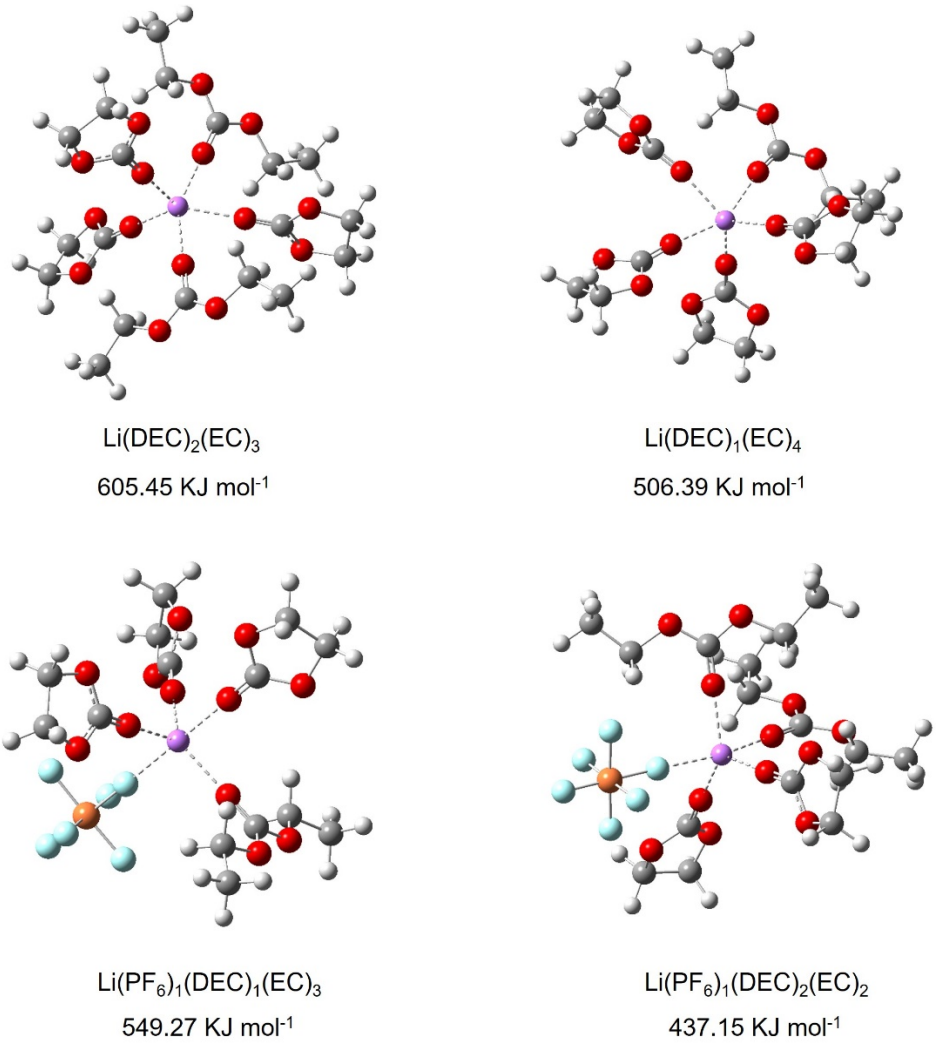

Fig. S12 The representative Li^+ solvation structures in the LE and their desolvation energy at -20 °C via DFT calculation.

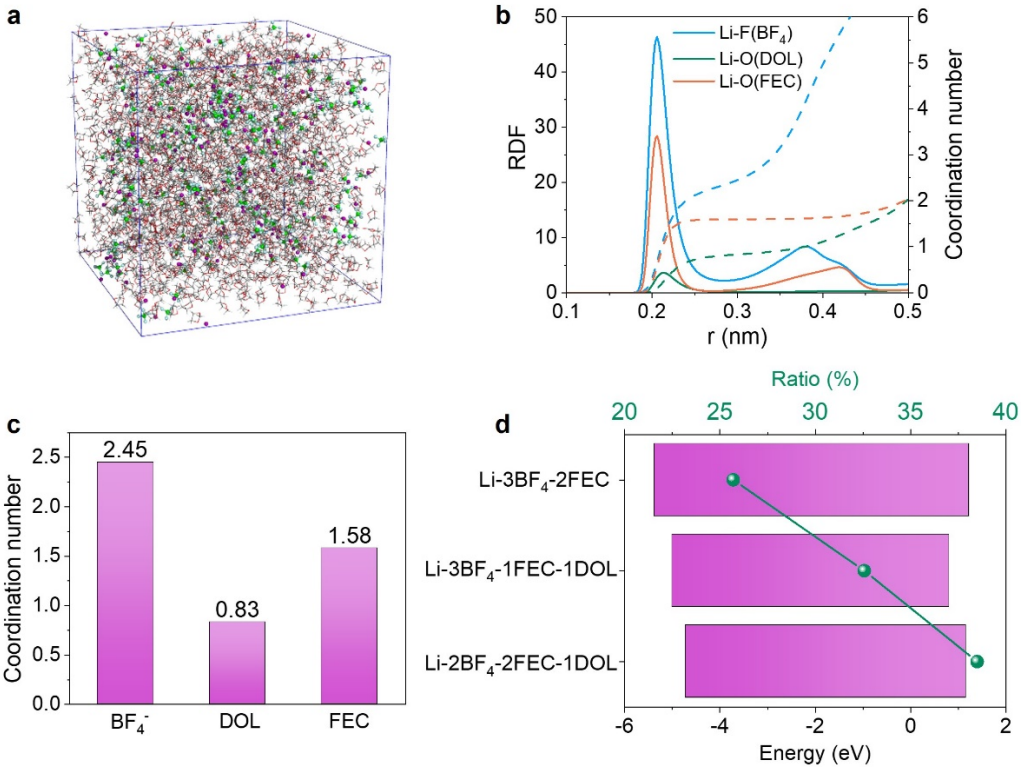

Fig. S13 a) Snapshots of the Li^+ solvation in the GPE precursor. **b**) The RDFs and CNs of the Li^+ solvation in the GPE precursor. **c**) The CNs between Li^+ and different electrolyte components for the GPE precursor. **d**) The ratio and orbital energy of the representative Li^+ solvation structure for the GPE precursor.

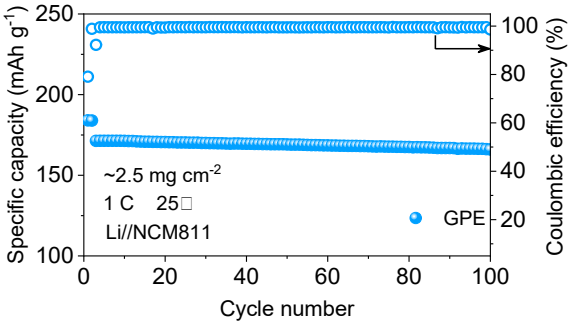

Fig. S14 Cycling performance of Li//NCM811 cells using the GPE at 1 C and 25 °C.

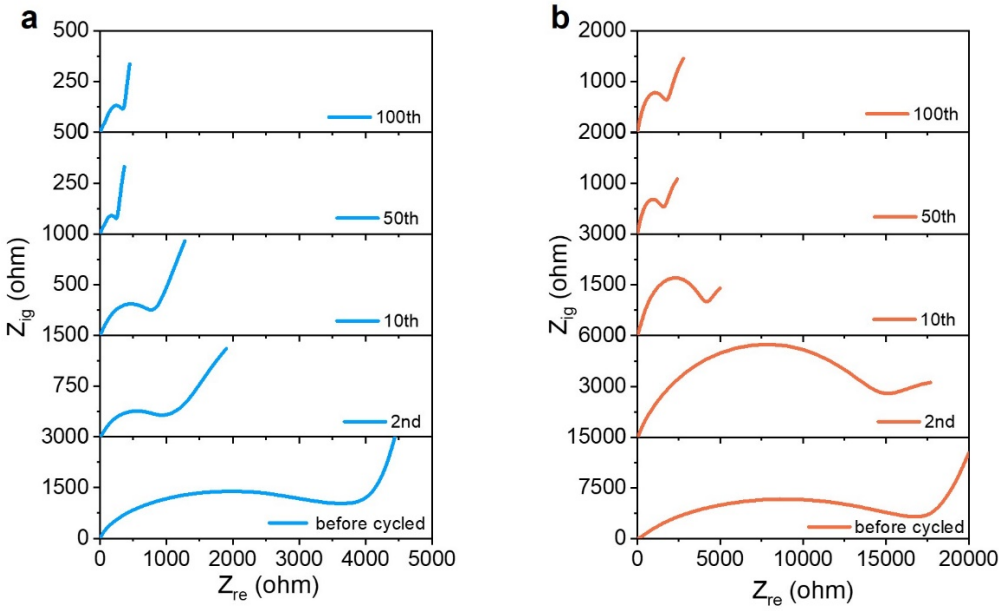

Fig. S15 ex situ EIS studies of different cycles for the Li//NCM811 cells for **a**) GPE and **b**) LE at -20 °C.

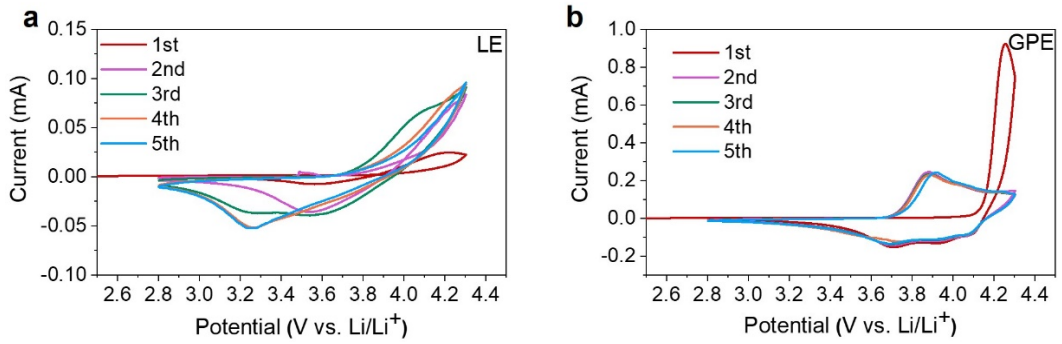

Fig. S16 CV curves of the **a**) LE and **b**) GPE at a scan rate of 0.1 mV s^{-1} from 2.8 to 4.3 V at -20 °C.

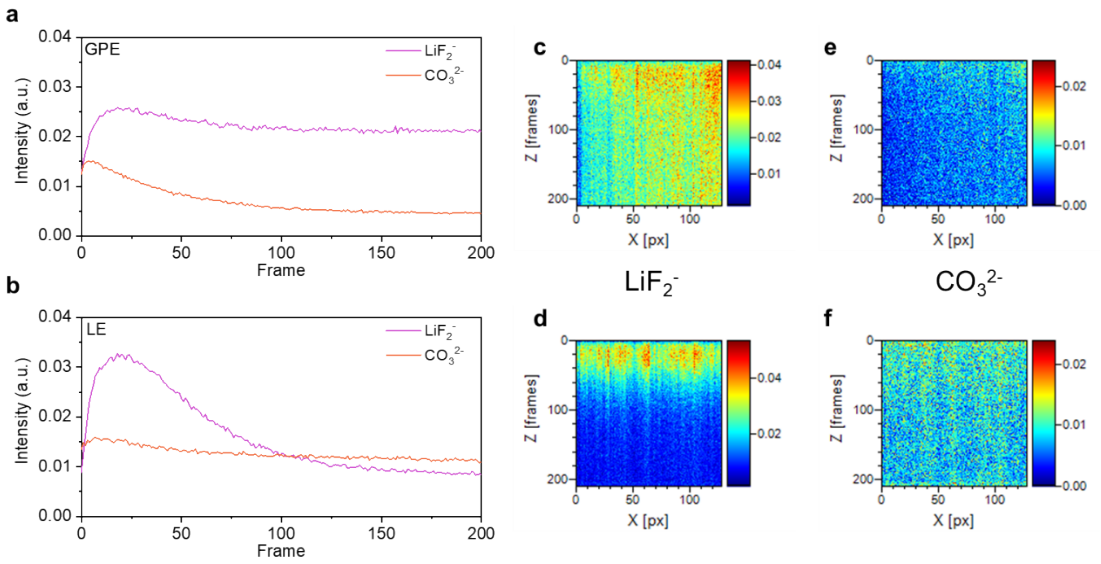

Fig. S17 TOF-SIMS depth profile of LiF_2^- and CO_3^{2-} of 50-cycled NCM811 cathodes for **a)** GPE and **b)** LE. LiF_2^- fragment mapping of 50-cycled NCM811 cathodes for **c)** GPE and **d)** LE. CO_3^{2-} fragment mapping of 50-cycled NCM811 cathodes for **e)** GPE and **f)** LE.

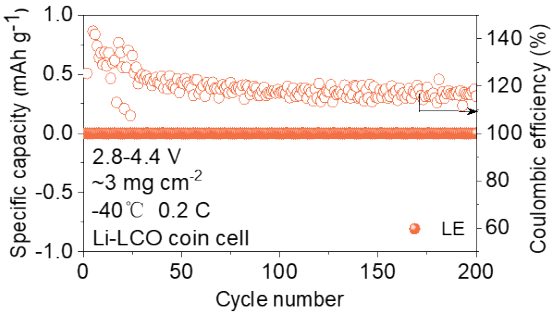

Fig. S18 Cycling performance of Li//LCO coin cell using the LE operating at 0.2 C under -40 °C.

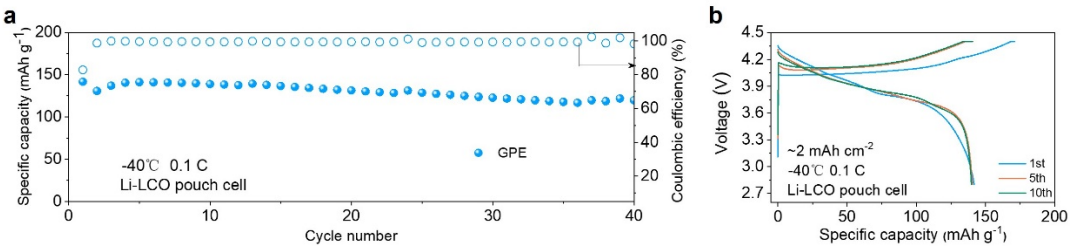

Fig. S19 a) Cycling performance of Li//LCO pouch cell using the GPE at 0.1 C under -40 °C. **b)** The corresponding charge-discharge curves of Li//LCO pouch cell at -40 °C in (**a**).

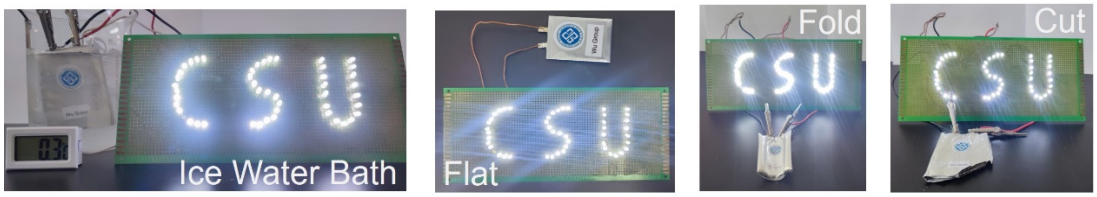

Fig. S20 The pouch cell lighting LEDs successfully after being placed in an ice water bath, folded or cut.

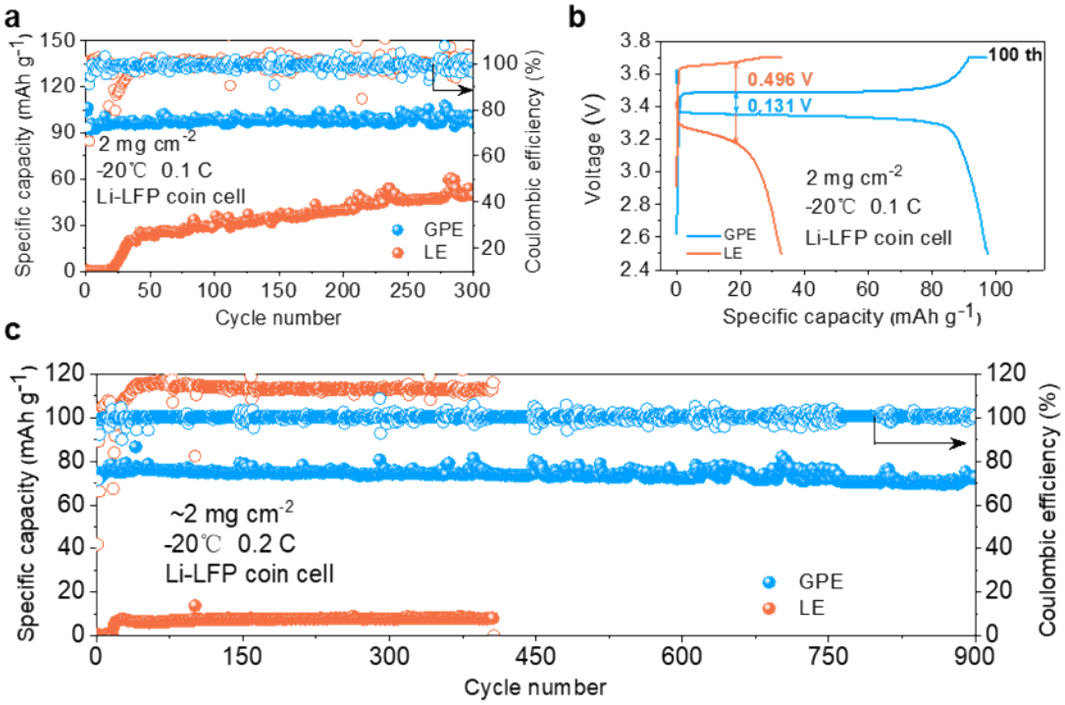

Fig. S21 Electrochemical performance of Li//LFP cells at low temperatures -20 °C. **a)** Cycling performance of Li//LFP cells using two electrolytes with mass loading of 2 mg cm^{-2} at 0.1 C and -20 °C. **b)** The corresponding charge-discharge curves of the 100th cycle in (a) for the two electrolytes. **c)** Cycling performance of Li//LFP cells using two electrolytes with mass loading of ~2 mg cm^{-2} at 0.2 C and -20 °C.

Table S1 Performance comparison of pouch cells of this work and reported GPE works at low temperatures.

pouch cell	temp. (°C)	rate (C)	discharge capacity (mAh g^{-1})	cycle numbers	Reference
Li//NCM811	-20	0.1	148	10	[1]
Li//NCM811	-30	0.1	94	10	[1]
Li//NCM811	-40	0.1	129	25	[2]
Li//LCO	-40	0.2	92	Not mentioned	[3]
Li//LCO	-20	0.1	161	50	This work
Li//LCO	-60	0.1	112	50	This work

Table S2 The detailed simulation system compositions in the three modeling systems.

No. of ion pairs/solvents	System1_GPE precursor	System2_GPE	System3_LE
Li-BF_4	200	200	
FEC	140	140	
DOL	1260	112	
PDOL4 (DOL tetramer)		287	
Li-PF_6			100
EC			750
DEC			412
Total No. of atoms	16460	17034	15716
Simulation system size	$(5.4403\ nm)^3$	$(5.5281\ nm)^3$	$(5.5074\ nm)^3$

References

1. Z. Li, R. Yu, S. Weng, Q. Zhang, X. Wang and X. Guo, *Nat. Commun.*, 2023, **14**, 482.
2. S. Mo, H. An, Q. Liu, J. Zhu, C. Fu, Y. Song and J. Wang, *Energy Storage Mater.*, 2024, **65**, 103179.
3. H. He, Y. Wang, M. Li, J. Y. Qiu, Y. H. Wen and J. H. Chen, *Chem. Eng. J.*, 2023, **467**, 143311.